



HAL
open science

Three consistent approaches of the multiple ckracking process in 1D composites

Étienne Castelier, Lionel Gélébart, Cécile Lacour, Christian Lantuéjoul

► **To cite this version:**

Étienne Castelier, Lionel Gélébart, Cécile Lacour, Christian Lantuéjoul. Three consistent approaches of the multiple ckracking process in 1D composites. *Composites Science and Technology*, 2010, 70 (15), pp.2146-2153. 10.1016/j.compscitech.2010.08.014 . hal-00557827

HAL Id: hal-00557827

<https://minesparis-psl.hal.science/hal-00557827>

Submitted on 24 Mar 2015

HAL is a multi-disciplinary open access archive for the deposit and dissemination of scientific research documents, whether they are published or not. The documents may come from teaching and research institutions in France or abroad, or from public or private research centers.

L'archive ouverte pluridisciplinaire **HAL**, est destinée au dépôt et à la diffusion de documents scientifiques de niveau recherche, publiés ou non, émanant des établissements d'enseignement et de recherche français ou étrangers, des laboratoires publics ou privés.

Accepted Manuscript

Three consistent approaches of the multiple cracking process in 1D composites

É. Castelier, L. Gélébart, C. Lacour, C. Lantuéjoul

PII: S0266-3538(10)00322-2
DOI: [10.1016/j.compscitech.2010.08.014](https://doi.org/10.1016/j.compscitech.2010.08.014)
Reference: CSTE 4795

To appear in: *Composites Science and Technology*

Received Date: 15 March 2010
Revised Date: 6 August 2010
Accepted Date: 21 August 2010



Please cite this article as: Castelier, É., Gélébart, L., Lacour, C., Lantuéjoul, C., Three consistent approaches of the multiple cracking process in 1D composites, *Composites Science and Technology* (2010), doi: [10.1016/j.compscitech.2010.08.014](https://doi.org/10.1016/j.compscitech.2010.08.014)

This is a PDF file of an unedited manuscript that has been accepted for publication. As a service to our customers we are providing this early version of the manuscript. The manuscript will undergo copyediting, typesetting, and review of the resulting proof before it is published in its final form. Please note that during the production process errors may be discovered which could affect the content, and all legal disclaimers that apply to the journal pertain.

Three consistent approaches of the multiple cracking process in 1D composites

É. Castelier*

CEA, DEN, SESC, F-13108 Saint-Paul-lez-Durance, France

L. Gélébart

CEA, DEN, SRMA, F-91191 Gif-sur-Yvette, France

C. Lacour, C. Lantuéjoul

MINESPARISTECH, 35 rue Saint Honoré F-77305 Fontainebleau France

Abstract

Most modellings found in literature for the multiple cracking process of 1D composites can be categorised into three different approaches: a continuous approach (CA) that assumes an infinitely long composite, and two random approaches that consider composites of finite length. The random strength approach (RSA) rests on a spatial discretization of the composite on which a strength distribution is applied, whereas the random crack approach (RCA) generates the location and the strength of each new crack without any discretization.

The first part of the paper lays the model and its statistical foundations. They are used to demonstrate that the three approaches should provide consistent results. The three approaches are then introduced, with special emphasis on the RCA as it is implemented for the first time without any approximation. Finally, the results provided by the three approaches are compared, confirming their full consistency.

Key words: A. Ceramic-matrix composites (CMCs), B. Fragmentation, C. Modelling, C. Probabilistic methods, B. Stress/strain curves

*Corresponding author

1. Introduction

Unidirectional composites, so-called micro- and mini-composites, are often used in the context of the development of Ceramic Matrix Composites. They consist of a single fibre (for micro-composites) or a single tow (for mini-composites) surrounded by a SiC matrix and an interphase (generally pyrocarbon for SiC/SiC composites) between the fibres and the matrix. The purpose of the interphase is to allow the deviation of a transverse matrix crack along the fibres. Thus, these 1D composites are generally used to devise optimal interphase features (thickness, chemistry...) to optimise their tensile behaviour. The quantification of this tensile behaviour requires the development of a model that accounts for the damage behaviour of the interphase and for the randomness of the multiple cracking stemming from the fragile behaviour of the matrix and the fibres. As a complete 3D model is prohibitive, unidirectional (1D) models have been considered in the literature. The main ingredients of these models are quite simple: the fragile matrix behaviour is given by the Weibull model [1] (or an alternative model) and the interphase behaviour is specified by a model of stress redistribution along the damaged interphase in the vicinity of a newly appeared crack.

Three different approaches are proposed in the literature to reproduce the behaviour of 1D composites:

- The first approach [2, 3, 4, 5, 6] consists in dividing the length of the 1D composite into a large number of small segments and to apply a random distribution of strengths. When the stress increases, cracks appear successively and the stresses are redistributed in their neighbourhood. Thus, the initial state is random, and then the evolution is strictly deterministic. Moreover, the results are independent of the segment lengths provided that they are small enough.
- The second approach [7, 8, 9] considers the 1D composite as an assembly

of fragments (portion of the 1D composite between two successive cracks) which become shorter and shorter as the stress increases and new cracks appear. Both the new crack location and the cracking stress are evaluated from statistical arguments based on the Weibull theory and on the stress distribution. Until now, all attempts to follow this approach have resorted to approximations.

- The third approach also considers the evolution of the fragment population but on an infinite 1D composite. From this assumption, the continuous distribution of fragment lengths can be analytically derived [10, 11].

In the following, these three approaches will be respectively referred to as the Random Strength Approach (RSA), the Random Crack Approach (RCA) and the Continuous Approach (CA).

The purpose of this paper is twofold. First, the RCA is presented for the first time free of any approximation. The second goal of this paper is to clarify and unify the different approaches proposed for modelling 1D composites. It is evidenced that the RCA (as implemented in the present paper) and the RSA provide the same statistical results as long as the RSA is performed with small enough segments. Such a comparison is all the more important because the equivalence of the RSA and the RCA was questioned in a recent paper [9]. Moreover, it is demonstrated that the statistical results provided by the RSA and the RCA tend to be identical to those provided by the CA as the micro-composite becomes very long.

For simplicity, an elementary model has been considered in this paper: the composite is a micro-composite, cracks occur only in the matrix according to Weibull's model, and the interphase behaviour is specified by a linear redistribution of stresses along the damaged interphase.

This model is firstly presented by focusing on the link between the spatial distributions of the flaws and the cracks. The three approaches are then presented with a special emphasis on our "exact" implementation of the RCA. Finally, the obtained results are compared and discussed.

2. Micro-Composite model

The micro-composite model under study has already been presented by several authors under different versions, the fragmentation occurring either in the fibre [7, 10] or in the matrix [12, 8]. The two versions yield expressions that are mathematically equivalent.

The key point of this model is the random crack process. As mentioned in [7, 10, 11], this process involves a population of flaws and a population of cracks. Flaws are inherent to the micro-structure of the brittle material, whereas cracks depend both on the flaw population and the stress history. The model is therefore presented in three parts: the flaw population, the mechanical stress profiles and the crack population.

2.1. Flaws and Weibull's model

A simple description of the spatial distribution of flaws is provided by Weibull's model. Hereunder is a presentation of this model and its probabilist interpretation (see also the paper by Henstenburg and Phoenix [7]).

Flaw space. A flaw in a 1D structure can be characterised by two parameters: its location $0 \leq x \leq L_0$ and its matrix strength $\sigma > 0$, *i.e.* the critical stress at which the flaw can turn into a crack. A flaw can therefore be seen as a random point (x, σ) of $[0, L_0] \times]0, \infty[$, called the *flaw space*, and the flaw population is a point process in the flaw space.

A classical result [13] is that the statistical properties of a point process are completely specified by its *avoidance function*. This function assigns each domain A of the flaw space the probability that the number $N(A)$ of flaws it contains is equal to zero (see Figure 1).

Poisson process. In a brittle material, the flaws can be assumed independent. In this case, they are distributed like a Poisson point process. Following [14], its avoidance function takes the form:

$$P\{N(A) = 0\} = \exp\left(-\int\int_A \lambda(x, \sigma) d\sigma dx\right), \quad (1)$$

where $\lambda(x, \sigma)$ is the intensity function of the process. There exists a simple interpretation for the Poisson intensity function. The mean number of flaws in the infinitesimal domain $dx d\sigma$ is equal to

$$E\{N(dx, d\sigma)\} = \lambda(x, \sigma)dx d\sigma. \quad (2)$$

Weibull's model. The original Weibull model [1] aims to predict the failure probabilities of a set of samples with same shape and size, submitted to a uniform tensile stress. Applied to the matrix, it gives the probability P that a slice with length l and cross-sectional area A_m holds under a stress σ_m :

$$P = \exp\left(-\frac{lA_m}{V_0}\left(\frac{\sigma_m}{\sigma_0}\right)^m\right),$$

The parameters of the Weibull's model are: the modulus m , a scale parameter σ_0 and a reference volume V_0 that often takes the value of $1m^3$. The matrix slice holds if it does not contain any flaw with an activation stress greater than σ_m , which can also be written:

$$P\{N([0, l] \times]0, \sigma_m]) = 0\} = \exp\left(-\frac{lA_m}{V_0}\left(\frac{\sigma_m}{\sigma_0}\right)^m\right). \quad (3)$$

This formula is an avoidance function applied to the domain $[0, l] \times]0, \sigma_m]$, corresponding to a Poisson process of intensity:

$$\lambda(x, \sigma_m) = \frac{mA_m}{V_0\sigma_0}\left(\frac{\sigma_m}{\sigma_0}\right)^{m-1}. \quad (4)$$

Note that the Poisson intensity is independent on the flaw location x , which means that the material is homogeneous. Flaws are uniformly distributed along the composite.

2.2. Stress distribution

When a micro-composite is increasingly loaded, the matrix gradually fails, producing more and more shorter and shorter fragments. The load becomes progressively transferred from the matrix to the fibre according to a stress redistribution mechanism that is presented now.

Sound material. A micro-composite is submitted to the mean stress σ . In the part of the composite far from any crack, the load is shared between the fibre and the matrix. The matrix and fibre stresses, σ_m and σ_f , are then proportional to the global stress:

$$\sigma_m = \varsigma_m \sigma, \quad \text{with} \quad \varsigma_m = \frac{E_m}{\bar{E}}, \quad (5a)$$

$$\sigma_f = \varsigma_f \sigma, \quad \text{with} \quad \varsigma_f = \frac{E_f}{\bar{E}}, \quad (5b)$$

where ϕ_m and ϕ_f respectively denote the volume fractions of the matrix and the fibre, E_m and E_f their Young modulus and $\bar{E} = \phi_f E_f + \phi_m E_m$ the mean Young modulus.

Slip zone. At a matrix crack location, the load is totally borne by the fibre whereas the matrix stress vanishes:

$$\sigma_m = 0, \quad \text{and} \quad \sigma_f = \frac{\sigma}{\phi_f}.$$

Moving from the crack, the stress is transferred along a slip zone from the fibre to the matrix. This transfer is modelled by an interfacial shear stress τ and is governed by the following differential equation:

$$\frac{\partial \sigma_m}{\partial x} = \frac{2 \tau \phi_f}{\phi_m R_f}, \quad (6)$$

where R_f denotes the fibre radius.

At both extremities of the slip zone, the matrix stress σ_m keeps its value $\varsigma_m \sigma$. The distance l_d from a crack to the sound zone is thus proportional to the stress σ :

$$l_d = \delta_m \sigma, \quad \text{with} \quad \delta_m = \frac{R_f \phi_m \varsigma_m}{2 \tau \phi_f}. \quad (7)$$

Accordingly, the composite can be divided into two zones: the slip zone and the sound zone.

Stress profiles. For a single crack, equation (6) shows that the matrix stress σ_m depends on the distance d to the crack:

$$\sigma_m = \frac{\varsigma_m}{\delta_m} d \quad \text{in the slip zone, for } d \leq \delta_m \sigma, \quad (8a)$$

$$= \varsigma_m \sigma \quad \text{in the sound zone, for } d \geq \delta_m \sigma. \quad (8b)$$

For a family of matrix cracks X_m , the matrix stress at location x depends on the distance $d(x, X_m)$ to the nearest crack:

$$\sigma_m(\sigma, x) = \varsigma_m \min\left(\frac{d(x, X_m)}{\delta_m}, \sigma\right). \quad (9)$$

The joint matrix and fibre stress profiles are schematically illustrated in Figure 2.

2.3. Cracks

During the loading of a composite, several flaws endure sufficient stress to be activated and transformed into cracks. Therefore the crack process results from the interaction between the spatial distribution of the flaws and the evolution of the stress profiles.

Next crack. A composite is loaded by letting the mean stress σ gradually increase. For a given load σ , the fragmentation state can be specified by the crack locations and the load σ_p of the previous crack. Figure 3 shows the matrix stress profile $\sigma_m(\sigma_p)$ corresponding to the previous crack. When the load σ increases, the matrix profile $\sigma_m(\sigma)$ moves upward, sweeping an increasing domain in the flaw space. The first flaw reached by the profile becomes a crack.

Screen effect. Let x be a point in the micro-composite situated at distance $d(x, X_m)$ from the nearest crack. According to Equation (7), it belongs to the slip zone as soon as

$$\frac{d(x, X_m)}{\delta_m} \leq \sigma. \quad (10)$$

In such a case, equation (9) shows that its matrix stress at x does not evolve:

$$\sigma_m(\sigma, x) = \varsigma_m \frac{d(x, X_m)}{\delta_m}. \quad (11)$$

Thus the matrix profile remains constant in the slip zone and cannot sweep new domains in the flaw space. No new flaw can be encountered, no new crack can occur in the slip zone. This *screen effect* has been identified by many authors [10, 15].

In the flaw space, inequality (10) defines a *screened domain* where flaws cannot be reached by the matrix stress profiles. The screened domain is a conic

domain for one crack, and a union of conic domains for several cracks (see Figure 3).

Crack search. Thus the encountered flaws are located in the sound zone where the matrix profiles gradually increase. The sweeping process can be simplified: sweeping the flaw space by increasing $\sigma_m = \varsigma_m \sigma$ (see Figure 3), the next crack corresponds to the first flaw discovered outside of the screened domain.

Saturation. During the loading the sound zone shrinks, both because of the expansion of the slip zones, and because of the occurrence of new cracks. It eventually vanishes at a *saturation* stress, say σ_{\max} . For greater stresses, the screen effect prevents the occurrence of any new crack.

2.4. Stress-strain curves

Stress-strain curves can now be derived from the model.

Stress. The mean stress balance equation

$$\sigma = \phi_f \sigma_f(\sigma, x) + \phi_m \sigma_m(\sigma, x),$$

together with the matrix stress profile (9) provides the fibre stress

$$\sigma_f(\sigma, x) = \frac{\sigma}{\phi_f} - \frac{\phi_m \varsigma_m}{\phi_f} \min\left(\frac{d(x, X_m)}{\delta_m}, \sigma\right). \quad (12)$$

Strain. For a given stress σ , the average strain of the micro-composite can be identified with that of the fibre:

$$\bar{\varepsilon}(\sigma) = \frac{1}{L_0} \int_0^{L_0} \frac{\sigma_f(\sigma, x)}{E_f} dx,$$

where L_0 is the composite length. Assuming that the composite has been divided into N fragments F_n , this average strain can be calculated by summing the elongation $\delta(\sigma, F_n)$ of each fragment:

$$\bar{\varepsilon}(\sigma) = \frac{1}{L_0} \sum_{n=1}^N \delta(\sigma, F_n), \quad \text{with} \quad \delta(\sigma, F_n) = \int_{F_n} \frac{\sigma_f(\sigma, x)}{E_f} dx.$$

It can also be viewed as the ratio of the average fragment elongation $\bar{\delta}(\sigma)$ to the average fragment length $\bar{l}(\sigma)$:

$$\bar{\varepsilon}(\sigma) = \frac{\bar{\delta}(\sigma)}{\bar{l}(\sigma)} \quad (13)$$

with

$$\bar{\delta}(\sigma) = \frac{1}{N} \sum_{n=1}^N \delta(\sigma, F_n) \quad \text{and} \quad \bar{l}(\sigma) = \frac{L_0}{N}.$$

The elongation $\delta(\sigma, F)$ of a fragment F depends on its length l and its location.

Explicitly, we have

$$\delta_i(\sigma, l) = \frac{\sigma}{E} \left[l + \frac{\phi_m E_m}{\phi_f E_f} \min \left(l - \frac{l^2}{4 \delta_m \sigma}, \delta_m \sigma \right) \right]$$

for a fragment between two cracks, and

$$\delta_e(\sigma, l) = \frac{1}{2} \delta_i(\sigma, 2l)$$

for a fragment between a crack and an extremity of the composite.

3. Three approaches of multiple cracking process

Starting from this modelling, three approaches are considered to derive the statistical properties of the cracking process:

- In the Random Strength Approach (RSA), the Poisson flaw intensity λ is used to assign random strength values on small slices along the discretized 1D composite (see Paragraph 3.1).
- In the Random Crack Approach (RCA), cracks are sequentially generated using a Monte Carlo method (see Paragraph 3.2).
- In the Continuous Approach (CA), an infinitely long 1D composite is considered. The continuous distribution of the fragment lengths has been analytically derived [11] (see Paragraph 3.3).

If properly implemented, these three approaches should yield similar results, as we shall see.

3.1. Random Strength Approach

The first approach has already been implemented in several studies [3, 5, 6].

Random strength. The matrix is discretized in small slices of thickness Δx . The strength Σ_m of each slice depends on its internal flaw population, and is thus random. Its distribution is given by Weibull's formula (3)

$$P\{\sigma_m < \Sigma_m\} = \exp \left[-\frac{A_m \Delta x}{V_0} \left(\frac{\sigma_m}{\sigma_0} \right)^m \right]. \quad (14)$$

According to the Poisson spatial distribution of the flaws, different slices contain independent flaw populations. Their respective random strengths are therefore independent.

Monte Carlo simulation. Following Rubinstein [16], a simple way to simulate random variables relies on uniform random variables on $[0, 1]$ as given by computers. If U is such a uniform variable, then a random variable X can be simulated using its *complementary cumulative distribution function* G :

$$X = G^{-1}(U), \quad \text{with} \quad G(x) = P(X > x). \quad (15)$$

Using Equation (14), a simulation of the random strength Σ_m of each slice is obtained by taking

$$\Sigma_m = \sigma_0 \left(-\frac{V_0 \ln(U)}{A_m \Delta x} \right)^{1/m}.$$

Evolution. At the beginning of the loading, the matrix stress is evaluated on each slice using equations (5). The loading is gradually increased till the matrix stress reaches the matrix strength of the weakest slice. Assuming the crack located in the middle of the slice, the stresses are then modified according to the stress profiles (9). The loading is again increased till a new crack is encountered, and so on until saturation.

Accuracy. The results nonetheless are sensitive to the slice thickness Δx . It must to be narrow enough to specify the stress profiles in the slip zones and localise the cracks accurately. A sensitivity analysis has been performed on

this parameter. It has been observed that a slice thickness less than 0.3% of the mean fragment length has negligible effects on results like the fragment histograms or the stress-strain curves (see Section 4).

In order to avoid further approximation, the loading is discretized according to the slice strength values and not regularly.

3.2. Random Crack Approach

The second approach simulates cracks sequentially using a Monte Carlo method. The main challenge of such approach is to simulate the cracks in their order of occurrence as the stress profiles evolve with the loading. In the many existing implementations of this approach [7, 8, 9], the loading σ is discretized with increments $\Delta\sigma$. Other simplifications [8, 9] can also be mentioned: the random Weibull distribution is transformed into a deterministic criterion, cracks are randomly or deterministically located along the composite, *etc.* The two algorithms presented here are new and rigorous, *i.e.* free of such approximations.

3.2.1. First algorithm

The first algorithm consists in searching sequentially all flaws and transforming into cracks only those that do not belong to the screened domain.

New flaw. If the previously detected flaw has a matrix strength σ_m^p , the matrix strength Σ_m of the new one is a random variable. Its value is greater of than σ_m if no other flaw belongs to the domain $[0, L_0] \times]\sigma_m^p, \sigma_m]$, which occurs with a probability given by Equations (1) and (4):

$$P\{\Sigma_m > \sigma_m\} = \exp\left(-\frac{L_0 A_m}{V_0 \sigma_0^m} [\sigma_m^m - \sigma_m^{p\ m}]\right). \quad (16)$$

The random variable Σ_m can then be simulated with the Monte Carlo method given by Equation (15):

$$\Sigma_m = \left(\sigma_m^{p\ m} - \ln U \frac{\sigma_0^m V_0}{L_0 A_m}\right)^{1/m} \quad (17)$$

where U is a uniform variable.

The location X of the new flaw is also random. According to [14], it is distributed proportionally to the Poisson intensity. In the present case, it is uniformly distributed over the composite.

Algorithm. We thus arrive to the following sequential algorithm. A saturation test is used at step (4) to terminate its execution.

- (1) Set $X_m = \emptyset$ (the crack set is empty) and $\sigma_m^p = 0$;
- (2) Simulate Σ_m using formula (17), and X uniform on L_0 ;
- (3) If (Σ_m, X) lies in the sound zone, then insert it to X_m ;
- (4) If the saturation stress has not been reached, then set $\sigma_m^p = \Sigma_m$ and go to (2);
- (5) Return X_m .

3.2.2. Second algorithm

Instead of examining all flaws, the second algorithm sequentially simulates only the flaws that turn into cracks. For each new crack, the load Σ at which it occurs and its location X have to be simulated.

New crack. Let σ_p be the composite load of the previous crack. The load Σ of the new crack is random, and its distribution can be specified using the flaw space described in Paragraph 2.3. Σ is greater than σ if no flaw lies in the domain swept by the matrix profile σ_m when the load varies from σ_p to σ (see Figure 3). According to Equation (1), this occurs with probability:

$$P\{\sigma < \Sigma\} = \exp(-H_{\sigma_p}(\sigma)), \quad (18a)$$

$$\text{with } H_{\sigma_p}(\sigma) = \int_{L_0} dx \int_{\sigma_m(\sigma_p, x)}^{\sigma_m(\sigma, x)} \lambda(x, s) ds. \quad (18b)$$

The distribution of Σ can then be simulated with the Monte Carlo method given by Equation (15):

$$\Sigma = H_{\sigma_p}^{-1}(-\ln(U)), \quad (19)$$

where U is a uniform variable. The inversion of H_{σ_p} can be achieved using Newton's method (cf. Appendix A).

Regarding the location of the new crack, X is uniformly distributed in the allowed domain, *i. e.* in the sound zone.

Algorithm. The algorithm for simulating the next crack is as follows:

- (1) Simulate the a standard uniform variable U ;
- (2) Calculate the random load Σ by applying Equation (19), using Newton's method for inverting Function H_{σ_p} ;
- (3) Simulate a uniform crack location X over the sound zone.

The crack process consists in simulating sequentially each new crack by this algorithm, until saturation.

Comparison. Both proposed algorithms have been numerically implanted and compared. They give the same results. For the rest of the paper, only Algorithm 2 has been used.

3.3. Continuous Approach

The third approach is an application of Hui *et al.* [11] formulae. As it is defined on infinitely long micro-composites, the length histograms of the fragments are in fact continuous probability density functions. Their evolution, during the fragmentation process, is governed by ordinary differential equations. The analytical solutions that are obtained can be viewed as mean results over a large number of composites of finite length.

Adaptation. In their paper, Hui *et al.* assumes that fragmentation takes place only in the fibre. In the present paper, fragmentation takes place only in the matrix. The swapping is achieved by modifying two dimensionality constants:

$$\sigma_c = \sigma_0 \left(\frac{V_0 \tau \phi_f}{A_m \sigma_0 R_f \phi_m} \right)^{\frac{1}{1+m}}, \quad (20a)$$

$$\delta_c = \frac{V_0}{A_m} \left(\frac{A_m \sigma_0 R_f \phi_m}{V_0 \tau \phi_f} \right)^{\frac{m}{1+m}}. \quad (20b)$$

Fragment population. Let f be the probability density function (p.d.f.) of the fragment lengths. For a mean stress σ , the proportion of fragments with length between l and $l + dl$ is $f(\sigma, l) dl$. The average of function g over all fragments is equal to:

$$\bar{g}(\sigma) = \int_0^{\infty} g(l) f(\sigma, l) dl. \quad (21)$$

Of course, it still depends on the stress σ applied to the composite.

Rather than the p.d.f. f , Hui *et al.* prefer using a density per unit length $p(\sigma, l)$ that is defined as:

$$p(\sigma, l) = f(\sigma, l) n(\sigma), \quad \text{with} \quad n(\sigma) = \frac{1}{\bar{l}(\sigma)}, \quad (22)$$

where $n(\sigma)$ denotes the crack density, that is the reciprocal of the fragment average length $\bar{l}(\sigma)$.

Density. Hui *et al.* found that the density p can be expressed as:

$$p(\sigma, l) \delta_c^2 = A_0(a) \exp(-xa^m) + 2m \int_a^b A_0(t) t^{-1} \exp\left[-\left(x + \frac{t}{2}\right) t^m\right] dt \quad (23)$$

It depends on two dimensionless parameters s and x that can be expressed using the constants introduced in (20):

$$s = \frac{\zeta_m \sigma}{\sigma_c}, \quad \text{and} \quad x = \frac{l}{\delta_c}$$

Moreover $a = \min(x, s)$, $b = \min(2x, s)$ and A_0 is the auxiliary function

$$A_0(s) = s^{2m} \exp\left(\frac{2m}{m+1} \int_0^{s^{m+1/2}} \frac{e^{-t} - 1 + t}{t} dt\right)$$

that can be numerically assessed using the special function Ein [17].

According to (22), the p.d.f. of the fragment lengths can be derived from the density p :

$$f(\sigma, l) = p(\sigma, l) \bar{l}(\sigma), \quad \text{with} \quad \frac{1}{\bar{l}(\sigma)} = \int_0^{\infty} p(\sigma, l) dl. \quad (24)$$

Mechanical behaviour. An important result which was not given by Hui *et al.* is the stress-strain curve of the composite. It can be derived from the density p .

According to (13), the average strain of a finite micro-composite is the ratio of the average fragment elongation $\bar{\delta}(\sigma)$ to the average fragment length $\bar{l}(\sigma)$. This relationship, independent of the composite size, extends to an infinitely long micro-composite:

$$\bar{\varepsilon}(\sigma) = \frac{\bar{\delta}(\sigma)}{\bar{l}(\sigma)} = \int_0^\infty \delta_i(\sigma, l) p(\sigma, l) dl. \quad (25)$$

The right-hand side of this equality is obtained by computing $\bar{\delta}(\sigma)$, using (21) and (24), the elongation considered being $\delta_i(\sigma, l)$ as given by (13).

Numerical implementation. The analytical formulae produced by Hui *et al.* are rather complex. They involve the special function Ein, and complex integrals. They can only be numerically implemented, which requires a mathematical library. We have used the GSL (GNU Scientific Library [18]) for this purpose.

4. Results

The implementations of the three aforementioned approaches are now compared. The parameters used for the tests are given in Table 1. They have been extracted from an paper of Guillaumat and Lamon [8] and refer to a SiC/SiC micro-composite.

Name	Symbol	Value	Unit
Fibre Proportion	ϕ_f	0.26	
Fibre diameter	$2 R_f$	15	μm
Length	L_0	2.5	cm
Matrix Young modulus	E_m	300	GPa
Fibre Young modulus	E_f	180	GPa
Shear stress	τ	5.	MPa
Weibull modulus	m	4.9	
Weibull scale parameter ($V_0=1 \text{ m}^3$)	σ_0	3.	MPa

Table 1: Parameters for a SiC/SiC micro-composite from Guillaumat and Lamon [8].

4.1. Mean results

The three approaches give results from different nature:

- The Random Strength and the Random Crack Approaches (RSA and RCA), simulate the fragmentation of a finite random composite using a Monte Carlo method. The results consist in a population of cracks. The size of the population varies from test to test.
- the Continuous Approach (CA) considers an infinite composite. The result is deterministic, namely the probability density function of the fragment lengths.

The continuous approach can be viewed as the result of a large number of simulations. It can be compared to the Monte Carlo approaches for the fragment histograms, or for the mechanical behaviour of the composite.

Histograms. Using the parameter set in Table 1, the Monte Carlo approaches produce very few fragments, about 8 or 9 at saturation. In order to compare statistical results with enough data, 10 000 tests have been performed. All fragments have been put together except those located at both extremities of the composite: they are statistically smaller than the others and must be discarded in order to avoid any edge effect.

Figure 4 presents the histograms obtained at saturation that have been produced by the two Monte Carlo Approaches. Both are compared to the theoretical probability density function provided by the Continuous Approach. There is an excellent agreement between the three approaches. The results provided by the both Monte Carlo approaches cannot be distinguished from a statistical point of view. From now on, the comparison will be made only between the Random Crack Approach and the Continuous Approach.

Mean behaviour. Using the Monte Carlo Approach, the micro-composite exhibits a random mechanical behaviour that varies from test to test. When N tests have been performed, an average behaviour can be computed. According

to the law of large numbers, this average behaviour becomes less and less random as N increases. This convergence to the mean is illustrated in Figure 5. The average of the traction curves performed over 1 and 10 tests are compared to the traction curve associated with the Continuous Approach. With enough tests performed, both curves are identical.

4.2. Ergodic behaviour

The average behaviour of many micro-composites coincides with the deterministic behaviour of an infinite micro-composite. This property is known as ergodicity: micro-composites gradually loses randomness as their size increases. This fact is illustrated in Figure 6 that plots the traction curves of composites with increasing lengths (in cm, $L_0 = 2.5, 25$ and ∞). This convergence versus the length L_0 is very similar to the convergence versus the number N that has been shown in Figure 5. The mean behaviour can be indifferently obtained by increasing either the number or the size of the composites.

Variance. It may be useful to assess the variability in the behaviour of a micro-composites as a function of its length. To do this, the crack density at saturation n_{sat} has been computed for several composite lengths. For each length, the crack density has been simulated for 1000 different random composites, then their average and their experimental variance have been computed. The average obtained coincides with the mean provided by the Continuous Approach: 346 cracks per metre.

Figure 7 shows that the experimental variance is inversely proportional to the composite length:

$$\text{var}(n_{\text{sat}}) \approx \frac{A}{L_0}, \quad (26)$$

The proportionality constant A has been satisfactorily fitted to a value around 29.

5. Discussion and conclusion

The three different approaches considered here have shown an excellent agreement. They are licit, free of any artifact and leads to similar results if

rigorously implemented. Their respective advantages and drawbacks are now discussed.

Random Strength Approach. The RSA is commonly used in failure mechanics, because its random and deterministic constituents can be treated separately. It easily generalises to 2D or 3D. For instance, Su *et. al.* [19] propose a 3D extension. At the initialisation step, random strength values are assigned to meshes using Weibull distribution. Then the finite element method is applied to achieve the mechanical calculations. In this example, the crack propagation is handled by cohesive zones.

For 1D composites, this approach is by far the less CPU-efficient. Furthermore it relies on an approximation: the mesh size Δx .

Continuous Approach. The CA provides analytical formulae. It is very convenient to directly derive information about the fragments distribution and the mean behaviour of the composite. An extension to non Weibull Poisson processes and non linear shear stress already exists [15], but it is doubtful that exact results can be obtained for more complex systems, such as mini-composites.

This approach applies to infinite micro-composites, thus providing the statistical mean behaviour of finite ones. But it does not give access to the actual variability that does exist in finite micro-composites.

Random Crack Approach. The RCA has already been applied to mini-composites [20], but approximations mentioned in section 3.2 have been introduced. Actually the straight implementation proposed in this paper for micro-composites can be extended to mini-composites. Compared to the RSA, it can be free of any approximation and extremely CPU-efficient.

Now it should be mentioned that the RCA becomes more and more difficult to implement as the complexity of the mechanical system increases. In particular, it does not seem so easy to implement in 2D or 3D.

A. Inversion using Newton scheme

Newton scheme is an iterative algorithm to invert a function F , by solving the implicit Equation:

$$y = F(x),$$

where x is the sought value. At Step k , a new value x^{k+1} is calculated from the current one x^k using the formula

$$x^{k+1} = x^k - \frac{F(x^k) - y}{F'(x^k)},$$

where F' denotes the derivative of F . The algorithm stops as soon as a specified accuracy has been reached.

References

- [1] W. Weibull, A statistical distribution function of wide applicability, *Journal of Applied Mechanics* 18 (3) (1951) 293–297.
- [2] W. A. Curtin, Fiber pull-out and strain localization in ceramic matrix composites, *Journal of the mechanics and physics of solids* 41 (1) (1993) 35–53.
- [3] C. Baxevanakis, D. Jeulin, D. Valentin, Fracture statistics of single-fibre composite specimens, *Composites science and technology* 48 (1–4) (1993) 47–56.
- [4] M. Ibnabdeljalil, S. L. Phoenix, Scalings in the statistical failure of brittle matrix composites with discontinuous fibers. I: Analysis and Monte Carlo simulations, *Acta metallurgica et materialia* 43 (8) (1995) 2975–2983.
- [5] C. Baxevanakis, D. Jeulin, J. Renard, Fracture statistics of a unidirectional composite, *International journal of fracture* 73 (2) (1995) 149–181.
- [6] A. T. diBenedetto, M. R. Gurvich, Statistical simulation of fiber fragmentation in a single-fiber composite, *Composites science and technology* 57 (5) (1997) 543–555.

- [7] R. B. Henstenburg, S. L. Phoenix, Interfacial shear strength studies using the single-filament-composite test. II: A probability model and Monte Carlo simulation, *Polymer composites* 10 (2) (1989) 389–408.
- [8] L. Guillaumat, J. Lamon, Fracture statistics applied to modelling the non-linear stress-strain behavior in microcomposites: influence of interfacial parameters, *International Journal of Fracture* 82 (1996) 297–316.
- [9] J. Lamon, Stochastic approach to multiple cracking in composite systems based on the extreme-values theory, *Composites science and technology* 69 (10) (2009) 1607–1614.
- [10] W. A. Curtin, Exact theory of fibre fragmentation in a single-filament composite, *Journal of materials science* 26 (19) (1991) 5239–5253.
- [11] C. Y. Hui, S. L. Phoenix, I. M., R. L. Smith, An exact closed-form solution for fragmentation of Weibull fibers in a single filament composite with applications to fiber-reinforced ceramics, *Journal of the Mechanics and Physics of Solids* 43 (10) (1995) 1551–1585.
- [12] W. A. Curtin, Multiple matrix cracking in brittle matrix composites, *Acta metallurgica et materialia* 41 (5) (1993) 1369–1377.
- [13] G. Matheron, *Random sets and integral geometry*, John Wiley & Sons, New York, 1975.
- [14] J. Kingman, *Poisson processes*, Clarendon Press, Oxford, 1993.
- [15] C. Y. Hui, S. L. Phoenix, L. Kogan, Analysis of fragmentation in the single filament composite: Roles of fiber strength distributions and exclusion zone models, *Journal of the Mechanics and Physics of Solids* 44 (10) (1996) 1715–1737.
- [16] R. Rubinstein, *Simulation and the Monte Carlo method*, Wiley, New York, 1981.

- [17] M. Abramowitz, I. A. Stegun, Handbook of Mathematical Functions with Formulas, Graphs, and Mathematical Tables, ninth Dover printing, tenth GPO printing Edition, Dover, New York, 1964.
- [18] M. Galassi, J. Davies, J. Theiler, B. Gough, G. Jungman, M. Booth, F. Rossi, Gnu Scientific Library: Reference Manual, 2nd Edition, Network Theory, 2003.
- [19] X. Su, Z. Yang, G. Liu, Monte Carlo simulation of complex cohesive fracture in random heterogeneous quasi-brittle materials: A 3d study, International Journal of Solids and Structures 47 (17) (2010) 2336–2345.
- [20] N. Lissart, J. Lamon, Damage and failure in ceramic matrix minicomposites: experimental study and model, Acta mater. 3 (1997) 1025–1044.

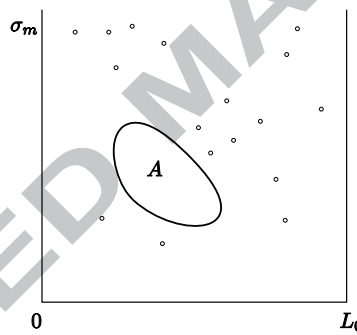


Figure 1: The probability that a domain A does not contain any flaw is called the avoidance function of A .

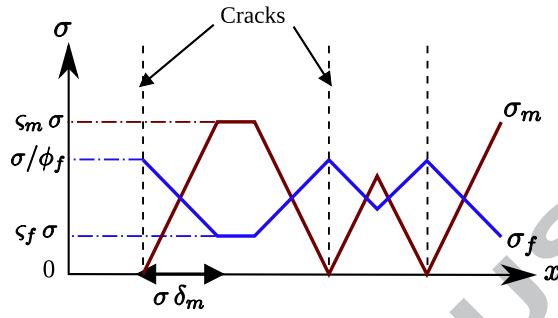


Figure 2: Stress profiles in the micro-composite.

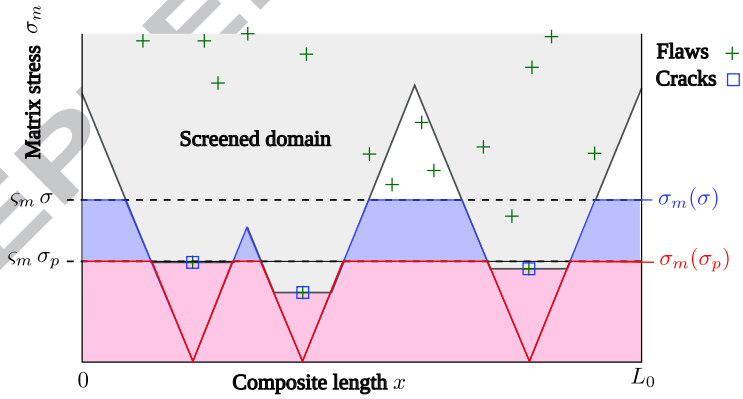


Figure 3: By increasing the load σ , the matrix profile $\sigma_m(\sigma)$ sweeps the flaw space. The next flaw reached by this profile corresponds to the next crack.

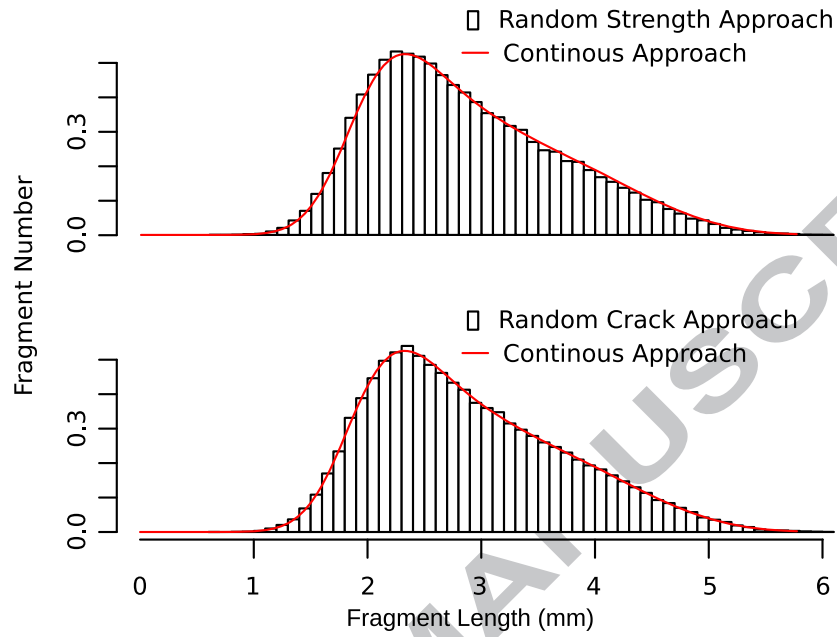


Figure 4: Comparison between both simulated histograms and the theoretical results of Hui *et al.*

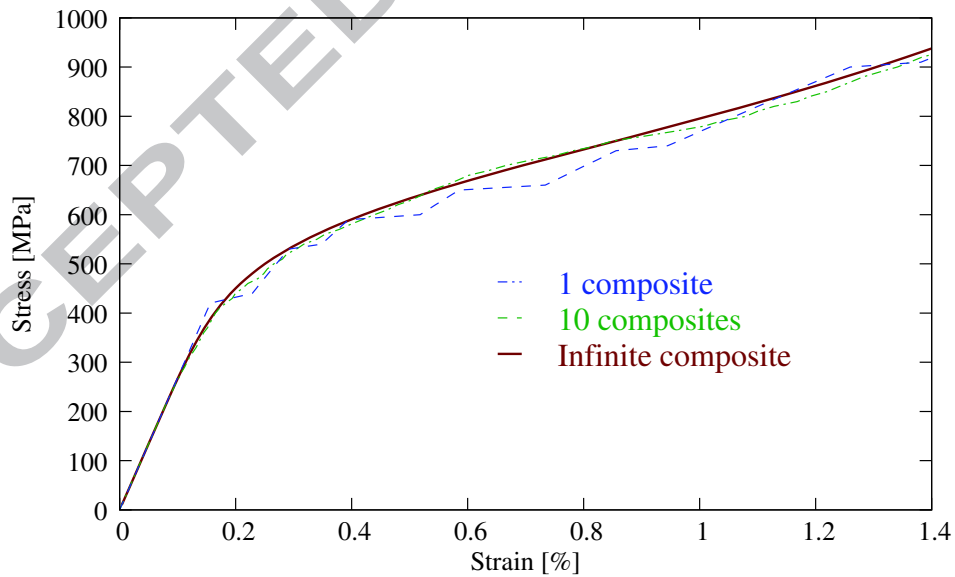


Figure 5: Convergence to the mean behaviour as a function of the number N of fragments.

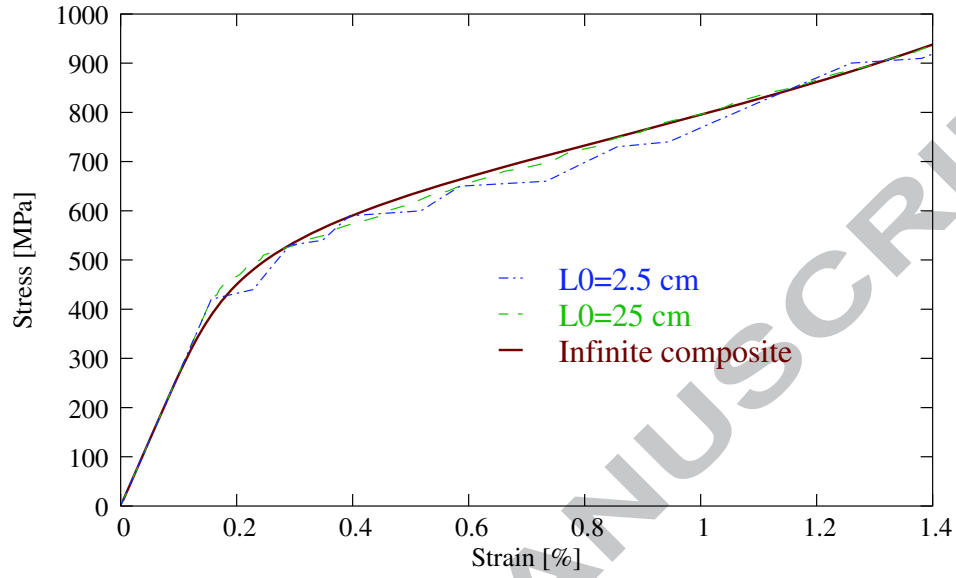


Figure 6: Convergence to the mean behaviour as a function of the length L_0 of the micro-composite.

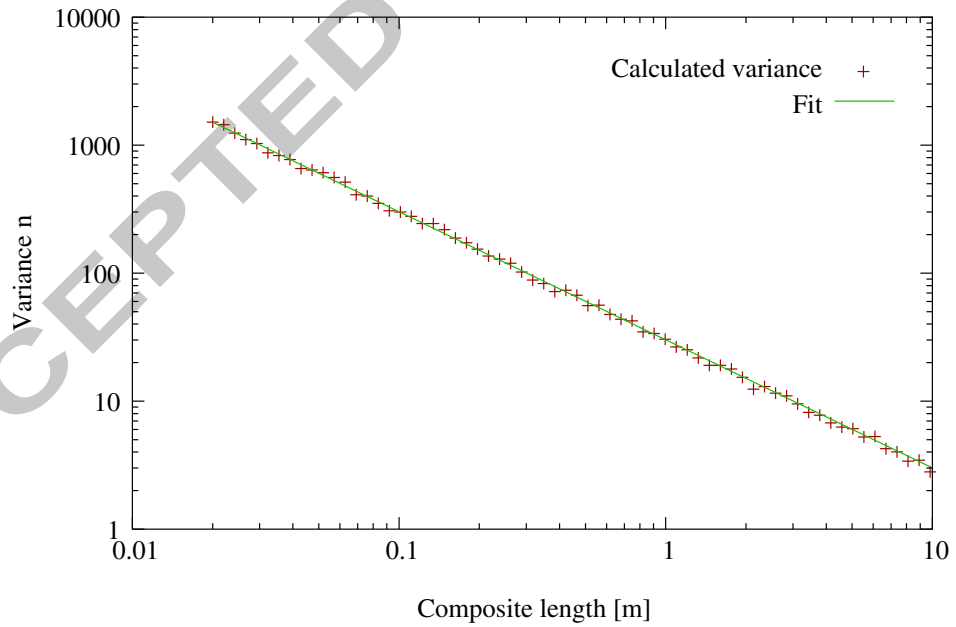


Figure 7: Variance of the crack density versus the composite length.